Evolution of passive margin escarpments: what can we learn from low-temperature thermochronology?

Jean Braun, Peter Van Der Beek

Evolution of passive margin escarpments: what can we learn from low-temperature thermochronology?

Jean Braun[1] & Peter van der Beek[2]

[1]Research School of Earth Sciences, The Australian National University, Canberra ACT 0200, Australia

[2]Laboratoire de Géodynamique des Chaînes Alpines, Université Joseph Fourier, Grenoble, France

July 29, 2004

Abstract

Recent studies integrating geomorphology, thermochronology, cosmogenic erosion rate estimates and numerical modeling suggest that escarpment evolution may take place following two dramatically different modes: (1) parallel retreat from the escarpment's original position at the continent-ocean boundary to its present-day inland position and (2) formation-in-place by progressive downwearing of a plateau initially located between the coast and a pre-existing inland drainage divide. Using a three-dimensional finite element model to solve the heat transfer equation, we show that the mode of migration of a passive margin escarpment can be constrained by low-temperature (apatite (U-Th)/He) thermochronology. We first couple the heat equation solver to a surface processes model that predicts the two different escarpment evolution modes from only slightly different initial conditions. We predict (U-Th)/He age distributions that are markedly different for the two scenarios; whereas a clear younging of ages from the coast to the escarpment characterizes the retreat mode, no such younging is observed in the downwearing mode. We perform a thorough investigation of the model behavior to determine under which circumstances thermochronological data can be used to constrain passive margin escarpment dynamics. We identify those conditions as those necessary to produce sufficient exhumation to reset the thermochronological system. They include (a) a tall escarpment, (b) a high geother-

mal gradient, and/or (c) a low flexural rigidity of the lithosphere. We demonstrate that, to determine the rate and mode of escarpment migration from low-temperature thermochronology, one needs to collect samples along transects perpendicular as well as parallel to the escarpment. Tightest constraints on escarpment development are provided by (in ascending order): the minimum age of the escarpment, the location of where the minimum age is found, the slope of the age-distance relationship (in a direction perpendicular to the coast) and the slope of the age-elevation relationship (from a transect parallel to the escarpment). We finally demonstrate that there are situations where thermochronological datasets do not provide constraints on the mode of escarpment migration, such as along the escarpment of southeastern Australia, where migration has possibly been very rapid. Using the Neighbourhood Algorithm method, we are, however, able to extract from an existing apatite (U-Th)/He dataset very useful constraints on the evolution of the southeastern Australian escarpment, including the duration of the migration event (< 15 Myr), the local geothermal gradient (32-40°C km^{-1}) and the effective elastic thickness of the underlying lithosphere (6-8 km).

Introduction

Passive margin escarpments are major geomorphic features that separate low-relief, high-elevation plateaus from near sea-level coastal plains. Their initial development is linked to a base level drop associated with the episode of continental rifting that leads to the opening of an oceanic basin. How they attain their present-day location from their original position, sometimes several hundred kilometers seaward, is a question that has been posed by geomorphologists for over a century (Suess, 1906; Penck, 1924; King, 1962) but remains a matter of debate (Gilchrist and Summerfield, 1990; ten Brink and Stern, 1992; Tucker and Slingerland, 1994; Gilchrist et al., 1994; Kooi and Beaumont, 1994; Seidl et al., 1996; Ollier and Pain, 1997; Cockburn et al., 2000; Bishop and Goldrick, 2000; van der Beek et al., 2002; Persano et al., 2002). Do escarpments retreat while maintaining their shape (Figure 1a), or do they evolve from their original position to the location of a pre-existing inland divide by degradation or downwearing of the continental plateau seaward of the divide

(Figure 1b). How do these high relief features survive for tens to hundreds of millions of years; in other words, how dynamic are they?

Much work has been done in recent years to constrain the rate of evolution of passive margin escarpments, such as those flanking the eastern Australian margin (Seidl et al., 1996; Heimsath et al., 2000, 2001; Persano et al., 2002) or the southern African margin (Fleming et al., 1999; Cockburn et al., 2000; Brown et al., 2002). These studies have integrated estimates of long-term denudation rates from low temperature thermochronometric methods, such as apatite fission track or (U-Th)/He thermochronology, with short-term erosion rate estimates from cosmogenic nuclides to provide more or less direct constraints on the rate of landform evolution.

The most recent of these studies (Cockburn et al., 2000; Persano et al., 2002; Brown et al., 2002) have concluded that escarpments do not evolve by simple 'linear' retreat of the original topographic step produced at the time of rifting. For the southeastern Australian escarpment, both apatite (U-Th)/He and fission-track ages are close to the estimated age of rifting in the Tasman Sea (Kohn et al., 2002; Persano et al., 2002; Persano, 2003), suggesting a rapid phase of denudation during or immediately after rifting. Available thermochronological ages in southernmost New South Wales do not show a clear pattern of younging from the coastline towards the escarpment, suggesting that following the rifting episode, the escarpment reached its present-day position rapidly, i.e. within 10 to 20 Myr, and has evolved only slowly since. These inferences are in accord with the occurrence of mid-Tertiary volcanic rocks and sediments only a few kilometers seaward of the escarpment, which indicate very slow rates of escarpment retreat over the last $\approx$ 30 Myr (Young and McDougall, 1982; Nott et al., 1991), as well as with cosmogenic data indicating slow escarpment retreat rates over $\approx 10^5$ yr timescales (Heimsath et al., 2000, 2001). Similar results have been obtained, and similar inferences drawn, for the escarpment on the southern African margins (Fleming et al., 1999; Cockburn et al., 2000; Brown et al., 2002).

The authors cited above have argued that the plateau degradation (or downwearing) model

(Figure 1a) is more consistent with the available thermochronological and cosmogenic data for these margins than the escarpment retreat model (Figure 1b). A retreating escarpment would progressively reset the thermochronological ages as it migrates from the coastline to its present-day position and therefore lead to a clear decrease in thermochronological ages from the coastline toward the escarpment. In both cases, however, the dataset remains relatively limited and many of the ages are similar to or older than the age of rifting, suggesting that exhumation since continental breakup and margin formation has not been sufficient to completely reset the apatite fission-track or (U-Th)/He ages.

Here, we propose to use a newly developed three-dimensional finite element model of heat transfer in the crust (Braun, 2002b, 2003) to determine how best to use low-temperature cooling ages, typically those obtained by the (U-Th)/He method in apatite, to constrain the evolution of a passive margin escarpment. In particular, we wish to determine: (a) under what conditions low-temperature chronology is likely to provide constraints on the nature and timing of escarpment evolution; (b) which aspects of this evolution can be constrained; and (c) what is the optimum sampling strategy (or strategies) that would produce the most useful constraints. Because our model is three-dimensional and optimized to predict the temperature field beneath a complex, time-varying surface topography, we can also estimate the importance of lateral heat transfer along high-elevation escarpments and its effect on the distribution of low-temperature cooling ages.

Although we recognize that there are several different models for the evolution of passive margin escarpments (Gallagher et al., 1998), we base our study here on whether thermochronological data can be used to differentiate between two of these models: Plateau Downwearing (PD Mode) versus Escarpment Retreat (ER Mode). To achieve this, we predict the temperature evolution of the crust beneath the escarpment assuming that one or the other evolutionary mode applies. From the time-varying temperature field, we predict the temperature-time histories of rocks that end up at the surface, from which apatite (U-Th)/He can be predicted. We estimate the sensitivity of

the thermochronological age distribution to varying model parameters, such as the height of the escarpment or its migration rate.

Heat transfer in the crust

In order to predict the distribution of thermochronological ages at the surface of the Earth from a given geomorphic scenario, we need to solve the heat transport equation, including conductive and advective terms as well as the effect of a time-varying surface topography. Three-dimensional heat transfer in the crust is governed by the following equation:

$$\rho_c c\left(\frac{\partial T}{\partial t} + \dot{E}\frac{\partial T}{\partial z}\right) = \frac{\partial}{\partial x}k\frac{\partial T}{\partial x} + \frac{\partial}{\partial y}k\frac{\partial T}{\partial y} + \frac{\partial}{\partial z}k\frac{\partial T}{\partial z} + \rho_c H \tag{1}$$

where T is temperature, t is time, x, y and z are the spatial coordinates, $\dot{E}$ is the vertical rock uplift rate (i.e., the velocity of rocks with respect to the fixed base at $z = -L$), k is conductivity, H is the rate of radiogenic heat production per unit mass, ρ_c is crustal density and c is heat capacity. Boundary conditions are:

$$T(z = -L) = T_L$$

$$T(z = S(x, y, t)) = T_{msl} + \beta z \frac{\partial T}{\partial n} = 0 \quad \text{on all side boundaries} \tag{2}$$

where $S(x, y, t)$ is the time-varying surface topography, T_{msl} is the assumed temperature at mean sea level and β is the atmospheric lapse rate. The initial temperature field is assumed to be at conductive equilibrium with a geometry that does not include the escarpment. To solve this equation we use the finite element code **Pecube** (Braun, 2003), which is designed to handle a finite-amplitude, time-varying surface topography. From the solution of this equation we can determine the temperature history of rock particles that will end up at the surface of the model at the end of the computations. From the thermal histories ($T - t$ paths) we compute (U-Th)/He ages in apatite, by using a finite difference scheme to solve the time-dependent, thermally-activated solid-state diffusion equation for Helium in apatite Wolf et al. (1998), for a large number of points at

the surface of the model.

In a high relief environment such as in the vicinity of a passive margin escarpment, lateral heat transfer cannot be neglected and requires the solution of the full three-dimensional heat transport equation, such as **Pecube**. This point is demonstrated in Appendix . Note that we have not included the thermal perturbation arising from the upwelling of hot mantle material associated with the stretching/extensional phase of rifting. The amplitude of such a perturbation is difficult to assess and will vary strongly from rift to rift, as it depends on the rate of extension, the width of the rift and the pre-rift geothermal gradient. We checked the effect of introducing a large thermal perturbation (400°C amplitude and 25 km half-width) near the rift axis on the age estimates and concluded that it did not have a substantial effect (apatite-He ages did not vary by more than 1%).

Coupling to Cascade

Pecube has been adapted to enable its coupling to the surface processes model **Cascade**(Braun and Sambridge, 1997), in which the evolution of surface topography with time is assumed to be governed by two dominant classes of mechanisms: long-range fluvial incision, transport and deposition, and local slope processes, including soil creep, overland flow and landsliding. **Cascade** has been used to integrate a range of geological, geophysical and thermochronological data to derive constraints on the evolution of the Southeastern Highlands of Australia (van der Beek and Braun, 1998, 1999; van der Beek et al., 1999), the escarpment of southeast Australia (van der Beek et al., 2001) and the Drakensberg escarpment of southeastern Africa (van der Beek et al., 2002). Coupling is achieved by imposing the evolving surface topography predicted by **Cascade** as the geometry of the imposed-temperature surface boundary of **Pecube**. The isostatic rebound predicted in **Cascade** is imposed through a spatially varying vertical rock uplift ($\dot{E}$) in **Pecube**.

To illustrate the potential use of thermochronological data in constraining the evolution of passive margin escarpments, we have used the predictions of two end-member **Cascade** model

runs from van der Beek et al. (2001) that predict escarpment evolution scenarios similar to the ER and PD modes of development from only slightly different initial conditions. The main difference between the two model runs is the presence, in the PD mode, of a low (100 m) pre-existing inland drainage divide, whereas an initially horizontal plateau leads to an ER Mode development. We impose a rather high geothermal gradient of $50°C \text{ km}^{-1}$, in order to maximize predicted differences in thermochronological ages, and a constant surface temperature of $0°C$. Both model runs were initiated 150 Myr ago and rifting took place 100 Myr ago. The results are shown in Figures 2 and 3.

Whereas the large-scale features of the final landscape predicted by the two models are very similar, the predicted (U-Th)/He apatite age distributions are markedly different (Figure 2). In the ER scenario, there is a clear progression from old ages (corresponding to the time of rifting) near the coast to young ages (corresponding to the time at which the escarpment stabilized at its present-day position) near the base of the escarpment (Figure 3). In the PD scenario, this progression does not exist; river incision and subsequent exhumation take place without a clear pattern of 'escarpment migration' and all ages are relatively old, close to the age of rifting (Figure 3). This example clearly demonstrates that, under some circumstances, the temperature structure within the upper crust, and, consequently, the distribution of low-temperature thermochronometric ages, are sensitive to the time evolution of the surface landform and, in particular, to whether a coastal escarpment migrated by retreat or by more uniform downwearing of an elevated plateau seaward of a pre-existing inland divide.

Parametric representation of surface evolution

We now simplify the surface evolution model and replace the predictions of the **Cascade** model with a parametric representation of each of the two scenarios. In the ER scenario, the escarpment is always the locus of the main drainage divide; it therefore propagates inland from its original position

along the continental margin without changing its shape. In the PD scenario, the main drainage divide is located inland from the original escarpment at the continental margin; the region between the initial coastal escarpment and the inland drainage divide is therefore progressively eroded away and a new escarpment forms at the location of the inland drainage divide.

In the ER scenario, the topography is calculated and imposed at the surface of the temperature solver according to the following expression:

$$z(x,y) = \frac{h}{2}\left(1 + \frac{2}{\pi}\arctan(\frac{x - x_m}{w})\right)$$
$$x_m = x_f \max(\frac{t}{t_f}, 1) + \frac{W}{10}\sin(5 \times \frac{2\pi y}{W}) \tag{3}$$

where t is time, h is the height of the original (and final) escarpment, w is the 'width' of the escarpment in the x-direction or direction of escarpment retreat, x_f is the final x-location of the escarpment and W is the length of the model in both x- and y-directions. It is assumed that the original escarpment (i.e., at the plate margin) formed at $x = 0$, 100 Myr ago (time $t = 0$ in the model). Its final position is the same in all model runs and for all scenarios considered. The time taken for the escarpment to reach its final position is a variable, t_f, which will determine the rate of migration of the escarpment, $v = \frac{x_f}{t_f}$. The escarpment is assumed to be incised by five river valleys of sinusoidal cross-section (Figure 1). These valleys represent the typical small-scale topographic relief observed along the face of many escarpments at a wavelength of approximately 10-15 km. The addition of this small scale relief will enable us to compute apparent exhumation rate from synthetic age-elevation relationships along the face of the escarpment. In the PD scenario, the surface topography linearly evolves from its original geometry:

$$z(x,y) = \frac{h}{2}\left(1 + \frac{2}{\pi}\arctan(\frac{x - x_m}{w})\right)$$
$$x_m = \frac{W}{10}\sin(5 \times \frac{2\pi y}{W}) \tag{4}$$

to its final geometry:

$$z(x, y) = \frac{h}{2}\left(1 + \frac{2}{\pi}\arctan(\frac{x - x_m}{w})\right)$$

$$x_m = x_f + \frac{W}{10}\sin(5 \times \frac{2\pi y}{W}) \tag{5}$$

The two scenarios are illustrated in Figure 1.

Finally, imposed changes in surface topography drive isostatic rock uplift and exhumation. This is computed by assuming that erosion of crustal rocks of density ρ_c leads to rebound of the underlying lithosphere that is regarded as a thin elastic plate of thickness T_e, elastic (Youngs) moduli Y and Poisson's ratio ν 'floating' on an inviscid substratum of density ρ_m.

The values of the model parameters are given in Table 1. We have performed a large number of model runs (approximately 5,000) in which five parameters were varied systematically. These are the escarpment height, h_0, the escarpment width, w, the time taken for the escarpment to reach its final position, t_f, the elastic plate thickness, T_e, and the escarpment evolution scenario (ER or PD). In order to compare rates of escarpment development more intuitively with the thermochronological ages, we introduce the 'stabilization time', $t_s = 100$ Myr - t_f and express it in geological time (i.e. Ma = Myr in the past). We have neglected the effects of the atmospheric lapse rate ($\beta = 0$) and the curvature to the geotherm introduced by the presence of heat generating elements in the crust ($H = 0$). Although we recognize that these parameters may affect the thermal structure of the crust, we have decided, for sake of clarity in our arguments, to neglect them in this parameter sensitivity analysis.

The predicted ages for one of the ER model runs are shown in Figure 4. There is a clear younging of the predicted ages from the coastline towards the escarpment. Oldest ages near the coast (82 Ma) are younger than the imposed time of base-level drop (100 Ma), whereas youngest ages (37 Ma) are somewhat older than the time at which the escarpment stabilized ($t_s = 25$ Ma) in this run. There is also a clear increase in age with elevation along the escarpment face and along the sides of the shorter wavelength valleys running in a direction perpendicular to the escarpment. The temperature field

beneath the escarpment shows how the surface topography affects the heat balance in the underlying crust (Figure 4). The short-wavelength valleys produce a temperature perturbation that does not penetrate beneath a few kilometers and, thus, does not affect the geometry of the 75°C isotherm. The escarpment, in contrast, induces a lateral temperature gradient that penetrates to the base of the model. All isotherms follow the long wavelength geometry of the escarpment (Figure 4). This is because the temperature anomaly caused by surface topography decreases exponentially with a skin depth equal to the wavelength of the topographic signal (Carslaw and Jaeger, 1959; Turcotte and Schubert, 1982).

We cannot present the predicted age distributions for all model runs; instead, we summarize the model results by computing, for each model run, (1) the minimum age, a_{min}, (2) the location (x_a) where the minimum age has been found, (3) the slope of the age-distance relationship along a profile perpendicular to the escarpment (between $x = x_a$ and $x = 0$), and (4) the apparent exhumation rate obtained by computing the gain between age and elevation along a profile parallel to the continental margin at $x = x_m$, at a wavelength equal to the imposed topographic wavelength of $W/5$ (see Braun (2002a) for a description of the method used to derive exhumation rate from age-elevation relationships along topographic transects). We use these results to (a) determine the conditions under which thermochronology can be used to constrain the style of escarpment evolution, (b) evaluate whether thermochronology can be used to differentiate between the two end-member scenarios for escarpment evolution, and (c) define the most practical way to extract the rate of escarpment migration from thermochronological data. We also provide constraints on the importance of lateral heat transport across the face of an escarpment.

Under what conditions can we use low-T (apatite-He) thermochronology to constrain escarpment evolution?

The time at which an escarpment first developed at the continental margin is linked to the time of continental rifting. In most cases, a minimum estimate for this time can be obtained from the oceanic magnetic anomaly pattern or by dating offshore sediments. A fundamental constraint for understanding the evolution of an escarpment and, more precisely, the rate at which it migrates inland, must be an estimate of the time at which it reached its present-day position. We investigate here under what conditions thermochronological ages from rocks collected in the coastal plain can provide such a constraint. In Figure 5, we present contour plots of the minimum apatite-He age (a_{min}) predicted in the various model runs as a function of the escarpment height (h_0) and stabilization time (t_s), for various values of the elastic plate thickness (T_e) and the two escarpment migration models (ER and PD). The minimum apatite-He age found in the coastal plain should be similar (and ideally identical) to the stabilization time. The initial, conductive geothermal gradient is the same in all model runs at 25°C km^{-1}; the width of the escarpment, w, is fixed at 5 km.

We see that for small elastic plate thickness, the minimum age is very similar to t_s, the stabilization time. For an 'average' value of the elastic plate thickness of 10 km, the minimum age is only an approximate measure of t_s for tall eascarpments ($h_0 > 2.5$ km). If the lithosphere is characterized by a thick effective elastic thickness ($T_e = 100$ km in our simulations), the minimum age is always much larger than the stabilization time, regardless of the escarpment height.

The main condition for observed ages to be closely related to the timing of the inland migration of the escarpment is that the latter should result in sufficient exhumation for rocks that are ultimately exposed at the surface to cross the closure temperature, T_c, of the thermochronological system. The maximum temperature experienced by rocks now exposed at the surface is:

$$T_{max} = E\frac{\partial T}{\partial z} \tag{6}$$

where E is the exhumation resulting from the migration of the escarpment. E is the sum of the height of the eroded escarpment, h_0, and the resulting isostatically-driven exhumation, h_i, which is a function of the flexural strength of the underlying lithosphere. For an infinitely weak lithosphere, one can assume local isostasy and the isostatic rebound is:

$$h_i^l = \frac{\rho_c}{\rho_m - \rho_c} h_0 \tag{7}$$

where ρ_c and ρ_m are the crustal and mantle densities, respectively. This value represents an upper bound for the isostatic rebound. For an infinitely rigid lithosphere, the isostatic rebound is nil and the exhumation is limited to the height of the eroded escarpment, $E = h_0$. This represents a lower bound for the total exhumation. The flexural strength of the lithosphere distributes the isostatic rebound over a horizontal length scale that is a function of the elastic thickness of the lithosphere and the wavelength of erosional unloading. The isostatic rebound caused by surface erosion of amplitude h_0 distributed over a wavelength w is given by (Turcotte and Schubert, 1982):

$$h_i = \frac{h_0}{\frac{\rho_m}{\rho_c} - 1 + \frac{D}{\rho_c g} \left(\frac{2\pi}{w}\right)^4} \tag{8}$$

where D is the flexural rigidity of the lithosphere, given by:

$$D = \frac{Y T_e^3}{12(1 - \nu^2)} \tag{9}$$

with Y Youngs modulus and ν Poissons ratio. The quantity $w_c = \left(D/\rho_c g\right)^{1/4}$ has the dimensions of a length and is commonly termed the 'natural flexural wavelength' of the lithosphere. Erosional unloading that takes place on a wavelength much shorter than w_c will not be accompanied by a substantial amount of isostatic rebound; erosional unloading on a wavelength greater than w_c will be fully isostatically compensated.

In our simulation, the wavelength of interest is the width of the coastal plain, w_p. In any model run, it evolves through time from 0 to $x_f = 37.5$ km, whereas the flexural wavelength varies, from one model run to the other, as a function of elastic plate thickness; $w_c = 4.2$ km, 24 km and 135 km, for $T_e = 1$ km, 10 km and 100 km, respectively. At the time of stabilization, the coastal

plain has reached its full width x_f. For $T_e = 1$ km, the width of the coastal plain is much greater than w_c, the system is very close to local isostasy and exhumation is approximately six times the height of the escarpment. For $T_e = 100$ km, the width of the coastal plain is much less than w_c, the lithosphere is strong enough to prevent isostatic rebound, and the exhumation is limited to the height of the escarpment. For intermediate values of T_e, isostatic rebound is only partial and comprised between 0 and 5 times the escarpment height. To reset (U-Th)/He ages in apatites, a system that has a closure temperature of $\approx 70°$C, requires approximately 2.4 km of exhumation for an initial geothermal gradient of 25°C km^{-1} and a surface temperature of 10°C. For a 1 km high escarpment, such an amount of isostatic rebound-driven exhumation is only achieved for a very low elastic plate thickness ($T_e = 1$ km) whereas a 3 km high escarpment produces sufficient exhumation even for more realistic elastic plate thicknesses ($T_e = 10 - 20$ km). These estimates are, of course, strongly dependent on the assumed geothermal gradient. The higher the gradient, the lower the exhumation and, hence, the lower the minimum initial escarpment height, required to exhume rocks with completely reset (U-Th)/He ages.

We can conclude that it is only in situations where the width of the region that has experienced denudation during the migration of the escarpment (w_p) is similar to or greater than the natural flexural wavelength of the lithosphere (w_c) that ages collected within the coastal plain will provide constraints on the development and migration of the escarpment. Furthermore, a relatively high geothermal gradient and/or low flexural rigidity is required to exhume reset ages for moderate-size escarpments ($h_0 \approx 1$ km), such as in southeastern Australia.

Can we differentiate between the two scenarios?

The most telling difference in model predictions between the two scenarios is the location, x_a, of the minimum age (Figure 6). In the ER scenario, the minimum age is always found near the present-day escarpment (i.e. in the range $x = 35 - 42$ km), whereas in the PD scenario, the minimum age

is found half-way between the coast and the escarpment (i.e. in the range $x = 22 - 28$ km). This is a first-order consequence of the exhumation pattern produced by each of the two scenarios. The ER scenario results in late exhumation near the foot of the escarpment whereas the PD scenario results in simultaneous exhumation at all locations within the coastal plain. In the PD scenario, the location of the age minimum is mostly affected by the isostatically-driven exhumation which, in all cases, is maximum at the centre of the region of erosional unloading, that is, half-way between the escarpment and the continental margin.

Intuitively, the ER scenario should also predict a clear pattern of younging of cooling ages from the continental margin towards the foot of the escarpment, followed by an increase in cooling ages from x_a across the escarpment towards the continental interior. The slope of the distance-age relationship from x_a to the margin should also contain information on the rate at which the escarpment migrated. Conversely, in the PD scenario, no such pattern should exist. In Figure 7, we present contour plots of the apparent migration rate of the escarpment, computed from the slope of the distance-age relationship from $x = x_a$ to $x = 0$. The slope is computed by linear regression of age versus distance. In all cases, the correlation coefficient is high ($> 85\%$). These estimates are compared to the imposed/true escarpment migration rate which is the ratio of the coastal plain width (37.5 km) and the time taken for the escarpment to propagate from the coast to its final position (t_f). In the ER scenario, there is a clear relationship between the slope of the distance-age relationship and the stabilization time, especially in cases where escarpment retreat leads to sufficient exhumation to reset the (U-Th)/He system (small T_e and tall escarpments). In all cases, however, the slope of the distance-age relationship overestimates the true escarpment retreat rate by at least a factor of 2, that is, the difference between a_{min} and the age at the continental margin is smaller than expected. This is again a consequence of the finite flexural strength of the lithosphere. When the escarpment evolves by progressive retreat, the width of the coastal plain increases with time. For a given elastic thickness T_e, the isostatically-driven exhumation will therefore be 'delayed' in the early stages of escarpment retreat until a time where the width of

the coastal plain, w_p, becomes comparable to the natural elastic wavelength, w_c. This effect will lead to a decrease of cooling ages near the margin and an apparent decrease of the difference in cooling ages between rocks at the coast and those at the foot of the escarpment. Moreover, in cases where exhumation is not sufficient to completely reset the thermochronological system, i.e. high T_e and/or low h_0, differences in ages across the coastal plain are decreased and the apparent propagation rate derived from distance-age relationship is wrongly amplified. Our computations clearly demonstrate that the slope of the distance-age relationship along a transect perpendicular to the escarpment can only be used to determine an upper bound to the escarpment migration rate.

Contrary to intuition, the model also predicts a clear pattern of younging of cooling ages from the margin towards the escarpment under the PD scenario. This is a consequence of the progressive isostatic-driven exhumation and its spatial distribution with respect to the centre of the region of erosional unloading. These results demonstrate that the presence of a clear age-distance relationship between the margin and the base of the escarpment cannot be used in itself to differentiate between the two scenarios.

What do we obtain from an age-elevation relationship?

Age-elevation relationships are commonly used to determine exhumation rates. This approach is particularly useful in situations where the isotherm corresponding to the closure temperature is not affected by the surface topography, in which case the slope of the age-elevation relationship is a direct measure of the local exhumation rate (Stüwe et al., 1994; Braun, 2002b). Under the PD scenario, local rates of exhumation should be relatively low and average around:

$$\dot{E}_{PD} = \frac{h_0 + h_i}{t_f} \tag{10}$$

whereas under the ER scenario, because a wave of exhumation migrates across the coastal plain with the retreating escarpment, local rates of exhumation at the escarpment should be much greater.

Maximum rates of exhumation can be estimated by scaling the mean denudation rates by a factor that equals the ratio of the width of the coastal plain to the width of the escarpment:

$$\dot{E}_{ER} = \frac{w_p}{w} \frac{h_0 + h_i}{t_f} \tag{11}$$

The escarpment itself is the only region affected by exhumation that has also preserves finite-amplitude topography where an estimate of the change in age with elevation can be obtained. We suggest comparing the exhumation rate obtained from the slope of an age-elevation profile sampled along the face of the escarpment with the 'mean' exhumation rate, obtained by dividing the height of the escarpment by the difference between the age of rifting and the minimum age measured in the coastal plain. If the escarpment has evolved by ER, the local exhumation rate at the escarpment should be much greater than the mean erosion rate. If the escarpment has evolved by PD, both estimates should be comparable.

To illustrate the point, we have computed a local exhumation rate from age predictions along a transect running along the face of the escarpment (i.e. parallel to the escarpment) at mid-elevations. We use the spectral method described by Braun (2002a) to estimate a gain value at the shortest available topographic wavelength (here 5 km). In Figure 8, we show contour plots of the ratio of that local erosion rate to a mean erosion rate obtained as explained above. The results clearly show that under the ER scenario, local exhumation rates are between 2 and 10 times greater than the first-order predictions from the escarpment migration rate, especially for slowly migrating escarpments (i.e. young stabilization ages). For the PD model, this ratio is between 1 and 3. This result demonstrates that age-elevation data collected at mid-elevations along a transect parallel to the escarpment can be very useful to determine the maximum recorded exhumation rate of the escarpment and, from that, the mode of escarpment migration.

Summary: Where to collect age data

In situations where exhumation has been sufficient to reset low-T systems (top panel in Figure 5), the minimum age observed on the coastal plain is a good indicator of the time at which the escarpment established itself in its present-day location and geometry. By collecting data along a transect from the base of the escarpment to the coast (or, ideally, to the edge of the continental margin), one should be able to constrain the rate of evolution of the escarpment (i.e. how rapidly it evolved from its initial to final positions) but not its mode of evolution (i.e. either by escarpment retreat or plateau downwearing). Age determinations along a transect parallel to the margin half-way up the escarpment provide an estimate of the local exhumation rate and, potentially, an independent constraint on the mode of escarpment evolution. These sampling strategies only apply to settings that experience sufficient exhumation to reset thermochronological systems. These settings include regions of high geothermal gradient, high elevation escarpment and/or those characterized by a low lithospheric flexural rigidity. Given the escarpment heights, flexural rigidities and geothermal gradients that characterize most high-elevation rifted margins, we would expect the apatite (U-Th)/He system ($T_c \approx 70°$C) to record differences in settings better, or more accurately, than apatite fission-track thermochronology ($T_c \approx 110°$C).

Application to the southeastern Australian escarpment

To illustrate our approach, we use the apatite (U-Th)/He data of Persano et al. (2002) from a transect across the southeastern Australian escarpment (Figure 9).

The eastern Australian margin developed as a result of oblique rifting in the Tasman Sea from ≈ 95 Ma onward, with oceanic spreading taking place in the Tasman Sea at ≈ 80 Ma (Gaina et al., 1998). The margin is characterized by an ≈1-km high escarpment running along its entire ≈2500-km length and separating a low-elevation coastal strip from a high-elevation but low-relief upland region. In southernmost New South Wales, where the data were collected (Figure 9), the

escarpment is cut into Paleozoic granites and metamorphic rocks and is located ≈35 km from the coast. In this area, the escarpment forms a secondary drainage divide between linear river systems that flow eastward to the Tasman Sea through relatively deeply incised valleys, and the Snowy River and its tributaries on the highland plateau, which flow away from the escarpment lip and then southward into Bass Strait (van der Beek and Braun, 1999). Short-term denudation rates have been determined from cosmogenic nuclides at a few tens of meters per million years on the coastal strip and < 10 m Myr^{-1} on the upland plateau (Heimsath et al., 2000, 2001). The occurrence of a volcanic plug (Mt. Dromedary), dated at 98 Ma, a few tens of kilometers north of Persano et al. (2002)'s transect indicates that the coastal strip existed in that area < 10 Myr after rifting started (Fabel and Finlayson, 1992).

Apatite (U-Th)/He ages were collected along a transect perpendicular to the escarpment in one of the major river valleys cutting up to it, the Bega Valley (Persano et al., 2002). Although most of the ages collected along the coastal strip are similar to or younger than the age of rifting at 85-95 Ma, they do not show any relationship with geographical position (i.e., distance to the coast or the escarpment) or elevation (Figure 10). This led Persano et al. (2002) to conclude that the present-day escarpment formed by either rapid retreat or so-called 'in-place' excavation (i.e. plateau degradation) soon after break-up.

As shown in the previous sections, however, many escarpment evolution scenarios can lead to apparently similar age distributions seaward of the escarpment. It is therefore interesting to determine whether the dataset collected by Persano et al. (2002) provides quantitative constraints on the mode of escarpment development. To achieve this, we have used our thermal-kinematic model to search for combinations of parameter values that would reproduce the observed age distribution. This search was performed by using the Neighbourhood Algorithm (NA) (Sambridge, 1999), a Monte-Carlo type inversion method that does not require the calculation of the derivatives of the forward model with respect to the model parameters. Instead, the NA method navigates

through the parameter space to find a minimum in the misfit function by making use of the natural neighbour and Voronoi diagram concepts. We have used the L_2-norm of the difference between the observation vector, O, and the prediction vector, P:

$$\text{misfit} = \frac{1}{n}\sqrt{\sum_i^n (O_i - P_i)^2} \tag{12}$$

where n is the number of measured ages (9 in our case).

In all model runs, the initial topography is assumed to be a perfectly flat plateau at a height of 1200 m above sea level. The final topography is the present-day topography as described by the 30 second global Digital Elevation Model, GTOPO30. We selected an area between $[149°\text{W}, 36.8°\text{S}]$ and $[150°\text{W}, 36.4°\text{S}]$ with 121 by 49 points used to represent the topography. All model runs last for 350 Myr. In all model runs, escarpment migration starts 100 Myr ago. We ran two types of scenarios, an Escarpment Retreat scenario where the transition from initial to final topography is progressively imposed from east to west, and a Plateau Downwearing scenario where the final topography is progressively and linearly carved out of the initial flat plateau. In both cases, we set the time taken to progress from the initial to the final topography as a free parameter between 15 and 85 Myr. The temperature at the base of the model, T_L, and the thickness of the thin elastic plate representing the flexural strength of the lithosphere, T_e, were selected as the other two free parameters and allowed to vary between 800 and 1500°C, and 1 and 100 km, respectively. The temperatures at the base of the model may seem unrealistically high but are only a result of our assumption of an initially linear geothermal gradient (between 23 and 43 °C km^{-1}) without heat production; they do not influence the model predictions.

The results are shown in Figure 11 as plots of the NA search in the $[T_e, T_L]$-parameter space. We do not show the search behaviour as a function of t_f as it rapidly converged to the shortest possible duration for the migration of the escarpment ($t_f = 15$ Myr). Each black dot corresponds to a model run. The large grey disks are the locations in parameter space of two local minima in the calculated misfit function. In both scenarios, the optimum elastic plate thickness varies

between 5 and 8 km and the optimum geothermal gradients between 32 and 40 °C km^{-1}. Optimum geothermal gradients are in good agreement with (sparse) heat-flow data for southeastern Australia that indicate a regional surface heat flow of $\approx$ 80 mWm^{-2} (Cull, 1982) (see also the Geoscience Australia online database at http://www.ga.gov.au/map/). The best-fit elastic plate thickness, in contrast, is significantly lower than the $T_e = 17$ km that was estimated by Zuber et al. (1989) for southeastern Australia from coherence analysis of topography and Bouguer gravity. Although there appears to be a trade-off between the elastic plate thickness and the basal temperature, with higher plate thicknesses requiring higher temperature gradients (and vice-versa) to obtain the same misfit, this trade-off is limited by the sharp increase in ages across the escarpment, which requires a relatively strong contrast in cooling and denudation histories for samples on either side of the escarpment. The smallest mean misfit is 7.4 Myr for the ER scenario and 6.8 Myr for the PD scenario.

Can different scenarios lead to the same age distribution?

In Figure 10 we compare the observed (U-Th)/He apatite ages of Persano et al. (2002) with the ages predicted under each of the two scenarios, using the model parameters yielding the smallest misfit. In the ER scenario, the optimum duration for escarpment migration is 15 Myr, the optimum elastic thickness is 5.4 km and the optimum geothermal gradient is 30°C km^{-1}. In the PD scenario, the optimum parameter values are 15 Myr, 6 km and 32°C km^{-1}, respectively. Figure 10 clearly demonstrates, as already concluded by Persano et al. (2002), that the existing low-temperature age data cannot be used to discriminate between the two proposed scenarios. The data are indicative of (a) a rapid propagation of the escarpment to its present-day position (necessary to predict ages in the coastal plain that are very close to the rifting age), (b) a relatively thin elastic thickness for the underlying lithosphere (necessary to reproduce the sharp transition in age across the escarpment face), and (c) a moderate to high geothermal gradient (necessary to reset the ages in the coastal

plain).

Interestingly, the two models predict very similar age distributions in the coastal plain (Figure 12), suggesting that there is little hope of determining which of the two scenarios is most appropriate for the area based on age determinations from the 'coolest' known thermochronological system. The reason for the lack of discriminative power in the thermochronological ages is that the escarpment migrated extremely rapidly to its present-day position.

A similar situation exists on the southeastern African margin, where apatite fission-track data from wells close to the Drakensberg escarpment face indicate a rapid cooling phase early in the history of the margin (Brown et al., 2002). This age pattern was interpreted by Brown et al. (2002) and modelled by van der Beek et al. (2002) as being most consistent with a Plateau Downwearing scenario for the development of the escarpment. Interestingly, based on independent (but possibly not very robust) geomorphic data, Partridge and Maud (1987) have also argued for a rapid early migration of the Drakensberg escarpment but favoured an Escarpment Retreat scenario, calling on climate change to explain the order-of-magnitude decline in retreat rates. As anticipated by van der Beek et al. (2002) and demonstrated here, the thermochronological data in themselves do not exclude such a scenario, but it is difficult to reproduce using numerical Landscape Evolution Models. We should therefore anticipate that a deeper understanding of the mode of escarpment evolution will not necessarily be attained through more data collection but from a better understanding of the actual processes causing escarpment retreat (e.g. Weissel and Seidl (1997, 1998)) and how rates of these processes may be affected by climatic variations.

Conclusions

Our modelling results lead us to the following conclusions :

- Because most passive margin escarpments have a finite height that is smaller than the exhumation required to reset the coldest of all thermochronometric systems, it is only in situations

where the width of the region that has experienced denudation during the migration of the escarpment (w_p) is similar or greater than the natural flexural wavelength of the lithosphere (w_c) that (U-Th)/He ages collected within the coastal plain will provide constraints on the development and migration of the escarpment.

- A relatively high geothermal gradient is required for moderate-height escarpments (1 km), and vice versa, in order to sufficiently reset thermochronological ages to be useful constraints on escarpment development.

- To discriminate between the two most commonly proposed scenarios (Escarpment Retreat or Plateau Downwearing) one needs to collect data along transects both perpendicular and parallel to the escarpment, from which age-distance or age-elevation relationships can be computed. These should, in turn, provide reasonable constraints on the rate of escarpment migration and the mode of migration, if the above conditions are respected.

- The value of the minimum age collected in the coastal plain is a reasonable first-order indicator (when compared to rifting age) of the rate of escarpment migration, although it tends to overestimate this rate. The location where the minimum age is observed is a function of the migration mode (ER or PD).

- Situations exist where the mode of escarpment migration cannot be constrained from thermochronological data. These typically occur when there has not been sufficient exhumation to completely reset the thermochronological system or, as is the case for the southeastern Australian escarpment, when the rate of propagation was such that only subtle differences in cooling ages are predicted from the two different scenarios.

- The results of our modelling of the dataset compiled by Persano et al. (2002) confirms their conclusion that it cannot be used to constrain the mode of escarpment migration in southeastern Australia. More importantly, the dataset contains information on the rate of escarpment

migration (fast), the lithospheric flexural strength (low) and the local geothermal gradient (moderate to high).

Acknowldegements

Three-dimensional heat transfer

To illustrate the effect of lateral heat transfer during escarpment migration, we compare the predicted ages for a typical model run with those obtained by imposing the condition that heat propagates conductively in the vertical direction only. Figure 13 shows contours of the relative difference in age between the two model runs. Differences are most important (nearly 40%) near the escarpment where the youngest ages are predicted. This demonstrates that accurate predictions of the evolution of the temperature field beneath an evolving escarpment require three-dimensional effects to be taken into account and that, in this environment, low temperature cooling ages such as those obtained from the (U-Th)/He system would be significantly affected by the approximation of one-dimensionality.

References

Bishop, P. and Goldrick, G. (2000). Geomorphological evolution of the East Australian continental margin. In Summerfield, M., editor, *Geomorphology and Global Tectonics*, pages 227–255, Chichester. John Wiley and Sons Ltd.

Braun, J. (2002a). Estimating exhumation rate and relief evolution by spectral analysis of age-elevation datasets. *Terra Nova*, 14:210–214.

Braun, J. (2002b). Quantifying the effect of recent relief changes on age-elevation relationships. *Earth and Planetary Sciences Letters*, 200:331–343.

Braun, J. (2003). Pecube: A new finite element code to solve the heat transport equation in three Dimensions in the Earth's crust Including the effects of a time-varying, finite amplitude surface topography. *Computers and Geosciences*, 29:787–794.

Braun, J. and Sambridge, M. (1997). Modelling landscape evolution on geological time scales: a new method based on irregular spatial discretization. *Basin Research*, 9:27–52.

Brown, R. W., Summerfield, M. A., and Gleadow, A. J. W. (2002). Denudational history along a transect across the Drakensberg Escarpment of southern Africa derived from apatite fission track thermochronology. *Journal of Geophysical Research*, 107:2350, doi:10.1029/2001JB000745.

Carslaw, H. S. and Jaeger, C. J. (1959). *Conduction of Heat in Solids*. Clarendon, Oxford, third edition.

Cockburn, H. A. P., Brown, R. W., Summerfield, M. A., and Seidl, M. (2000). Quantifying passive margin denudation and landscape development using combined fission-track thermochronology and cosmogenic isotope analysis. *Earth and Planetary Sciences Letters*, 179:429–435.

Cull, J. (1982). An appraisal of australian heat-flow data. *BMR Journal of Australian Geology and Geophysics*, 7:11–21.

Fabel, D. and Finlayson, B. L. (1992). Constraining variability in south-east Australian long-term denudation rates using a combined geomorphological and thermochronological approach. *Zeitschrift fr Geomorphologie Neues Folge*, 36:293–305.

Fleming, A., Summerfield, M. A., Stone, J. O. H., Fifield, L. K., and Creswell, R. G. (1999). Denudation rates for the southern Drakensberg escarpment, SE Africa, derived from in-situ-produced cosmogenic ^{36}CL: initial results. *Journal of the Geological Society of London*, 156:209–212.

Gaina, C., Mller, D. R., Royer, J.-Y., Stock, J., Hardebeck, J., and Symonds, P. (1998). The tectonic history of the Tasman Sea: A puzzle with 13 pieces. *Journal of Geophysical Research*, 103(B6):12,413–12,434.

Gallagher, K., Hawkesworth, C., and Gleadow, A. J. W. (1998). The denudation history of the onshore continental margin of s.e. brazil inferred from fission track data. *Journal of Geophysical Research*, 99:18,117–18,145.

Gilchrist, A. R., Kooi, H., and Beaumont, C. (1994). Post-Gondwana geomorphic evolution of southeastern Africa: implications for the controls on landscape development from observations and numerical experiments. *Journal of Geophysical Research*, 99:12221–12228.

Gilchrist, A. R. and Summerfield, M. A. (1990). Differential denudation and flexural isostasy in the formation of rifted-margin upwarps. *Nature*, 346:739–742.

Heimsath, A. M., Chappell, J., Dietrich, W. E., Nishiizumi, K., and Finkel, R. C. (2000). Soil production on a retreating escarpment in southeastern Australia. *Geology*, 28:787–790.

Heimsath, A. M., Chappell, J., Dietrich, W. E., Nishiizumi, K., and Finkel, R. C. (2001). Late Quaternary erosion in southeastern Australia: a field example using cosmogenic nuclides. *Quaternay International*, 83(5):169–185.

King, L. (1962). *The Morphology of the Earth.* Oliver & Boyd, Edinburgh/London.

Kohn, B. P., Gleadow, A. J. W., Brown, R. W., Gallagher, K., O'Sullivan, P. B., and Fosrter, D. A. (2002). Shaping the Australian crust over the last 300 million years: insights from fission track thermotectonic imaging and denudation studies of key terranes. *Australian Journal of Earth Sciences*, 49:697–717.

Kooi, H. and Beaumont, C. (1994). Escarpment evolution on high-elevation rifted margins: insights derived from a surface processes model that combines diffusion, advection and reaction. *Journal of Geophysical Research*, 99:12,191–12,209.

Nott, J. F., Idnurm, M., and Young, R. W. (1991). Sedimentology, weathering, age and geomorpho-logical significance of Tertiary sediments on the far south coast of New South Wales. *Australian Journal of Earth Sciences*, 38:357–371.

Ollier, C. D. and Pain, C. P. (1997). Equating the basal unconformity with the palaeoplain: a model for passive margins. *Geomorphology*, 19:1–15.

Partridge, T. C. and Maud, R. R. (1987). Geomorphic evolution of southern Africa since the Mesozoic. *South African Journal of Geology*, 90:179–208.

Penck, W. (1924). *Die Morphologische Analyse: Ein Kapital der Physikalischen Geologie.* Engel-horn, Stuttgart.

Persano, C. (2003). *A combination of apatite fission track and (U-Th)/He thermochronometers to constrain the escarpment evolution in south eastern Australia : a case study of high elevation passive margins.* PhD thesis, University of Glasgow.

Persano, C., Stuart, F. M., Bishop, P., and Barford, D. N. (2002). Apatite (U-Th)/He age con-straints on the development of the Great Escarpment on the southeastern Australian passive margin. *Earth and Planetary Sciences Letters*.

Sambridge, M. (1999). Geophysical Inversion with a Neighbourhood Algorithm -I. Searching a parameter space. *Geophysical Journal International*, 138:479–494.

Seidl, M. A., Weissel, J. K., and Pratson, L. F. (1996). The kinematics and pattern of escarpment retreat across the rifted continental margin of SE Australia. *Basin Research*, 12:301–316.

Stüwe, K., White, L., and Brown, R. (1994). The influence of eroding topography on steady–state isotherms. Application to fission track analysis. *Earth and Planetary Sciences Letters*, 124:63–74.

Suess, E. (1906). *The Face of the Earth (Vol. 2)*. F. Tempsky, Vienna.

ten Brink, U. S. and Stern, T. (1992). Rift-margin uplifts and flexural inland basins: Comparison between the Transantarctic Mountains and the Great Escarpment of southern Africa. *Journal of Geophysical Research*, 97:569–585.

Tucker, G. E. and Slingerland, R. L. (1994). Erosional dynamics, flexural isostacy, and long-lived escarpments: A numerical modeling study. *Journal of Geophysical Research*, 99:12,229–12,243.

Turcotte, D. L. and Schubert, G. (1982). *Geodynamics: Applications of Continuum Physics to Geological Problems*. John Wiley and Sons, New York, first edition.

van der Beek, P. and Braun, J. (1998). Numerical modelling of landscape evolution on geological time scales: a parameter analysis and comparison with the southeastern highlands of Australia. *Basin Research*, 10:49–68.

van der Beek, P. and Braun, J. (1999). Controls on post-mid-Cretaceous landscape evolution in the southeastern highlands of Australia: insights from numerical surface process models. *Journal of Geophysical Research*, 104:4945–4966.

van der Beek, P., Braun, J., and Lambeck, K. (1999). Post-Palaeozoic uplift history of southeastern Australia revisited: results from a process-based model of landscape evolution. *Australian Journal of Earth Sciences*, 46:157–172.

van der Beek, P., Pulford, A., and Braun, J. (2001). Cenozoic landscape evolution in the Blue Mountains (SE Australia): Lithological and tectonic controls on rifted margin morphology. *Journal of Geology*, 109:35–56.

van der Beek, P., Summerfield, M., Braun, J., Brown, R., and Fleming, A. (2002). Modelling post-breakup landscape development and denudational history across the southeast African (Drakensberg Escarpment) margin. *Journal of Geophysical Research*, 107:2351, doi:10.1029/2001JB000744.

Weissel, J. K. and Seidl, M. A. (1997). Influence of rock strength properties on escarpment retreat across passive continental margins. *Geology*, 25:631–634.

Weissel, J. K. and Seidl, M. A. (1998). Inland propagation of erosional escarpments and river profile evolution across the southeast Australian passive continental margin. In Tinkler, K. J. and Wohl, E. E., editors, *Rivers over Rock: Fluvial Processes in Bedrock Channels*, pages 189–206. Geophysical Monograph 107. American Geophysical Union.

Wolf, R. A., Farley, K. A., and Kass, D. M. (1998). Modeling of the temperature sensitivity of the apatite (U-Th)/He thermochronometer. *Computers and Geosciences*, 148:105–114.

Young, R. W. and McDougall, I. (1982). Basalts and silcretes on the coast near Ulladulla, southern New South Wales. *Journal of the Geological Society of Australia*, 29:425–430.

Zuber, M., Bechtel, T., and Forsyth, D. (1989). Effective elastic thickness of the lithosphere and mechanisms of isostatic compensation in Australia. *Journal of Geophysical Research*, 94:9353–9367.

List of Figures

a) Escarpment Retreat (ER)   b) Plateau Degradation (PD)

Figure 1: Two end-member models for the inland migration of a passive margin escarpment initially formed by a rapid base level fall associated with continental rifting and the formation of an ocean basin. (a) Escarpment retreat (ER) scenario; (b) Plateau downwearing (PD) scenario.

Figure 2: Landform predicted by **Cascade** and apatite (U-Th)/He age distribution predicted from **Pecube** temperature estimates under the two end-member scenarios. Geothermal gradient of 50°C/km and a constant surface temperature of 0°C. The runs started 150 Myr ago and rifting took place 100 Myr ago in both model scenarios. In the ER model there is a clear pattern from old ages at the margin to young ages at the foot of the escarpment. In the PD model, ages are consistantly older and do not show a clear younging trend towards the escarpment.
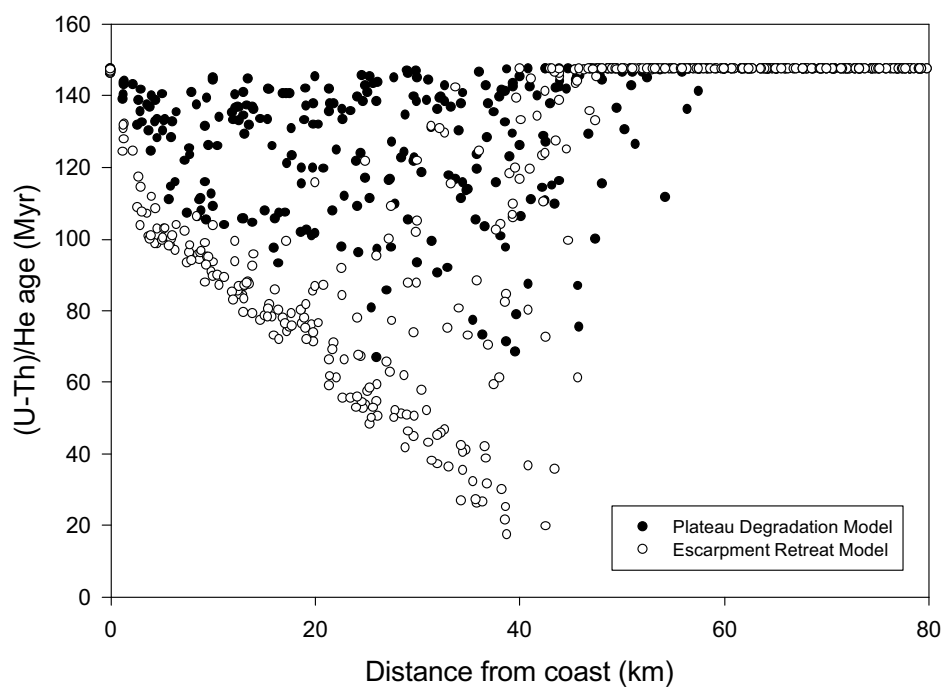
Figure 3: Distribution of apatite (U-Th)/He ages as a function of distance from the coastline as computed from **Pecube** temperature predictions under the two end-member scenarios.
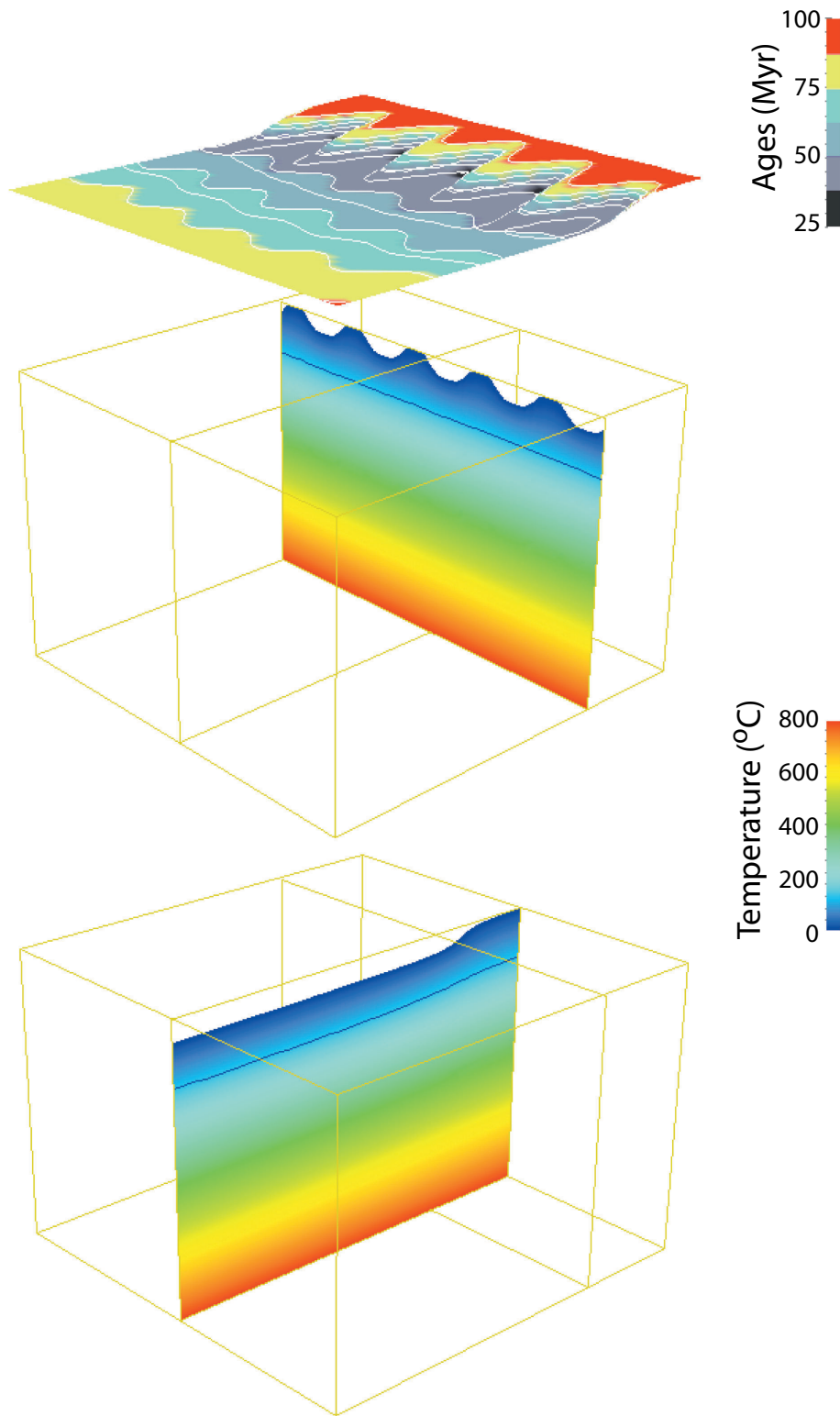
Figure 4: Computed apatite (U-Th)/He ages for one of many model runs draped over the final surface topography and underlying temperature distribution along two orthogonal cross sections. The thin solid line is the 75°C isotherm. Parameters are: $h_0 = 3$ km, $w = 2$ km, $t_f = 75$ Myr, $T_e = 10$ km; model scenario is ER.
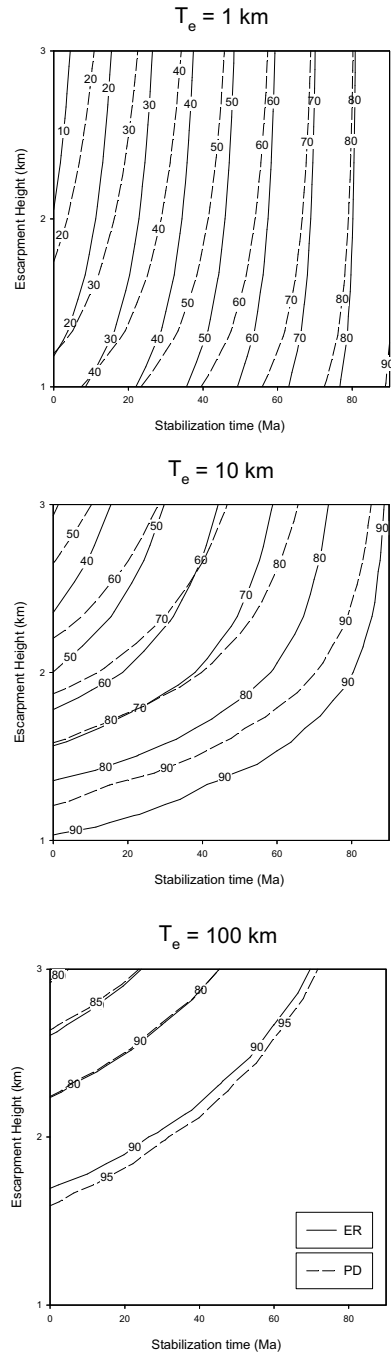
Figure 5: Predicted minimum apatite-He age as a function of escarpment height, h_0, and stabilization time, t_s, for three values of the assumed elastic plate thickness, T_e, and a breakup age of 100 Ma.

Continuous lines represent results for the Escarpment Retreat (ER) mode of escarpment development; dashed lines for the Plateau Downwearing (PD) mode.
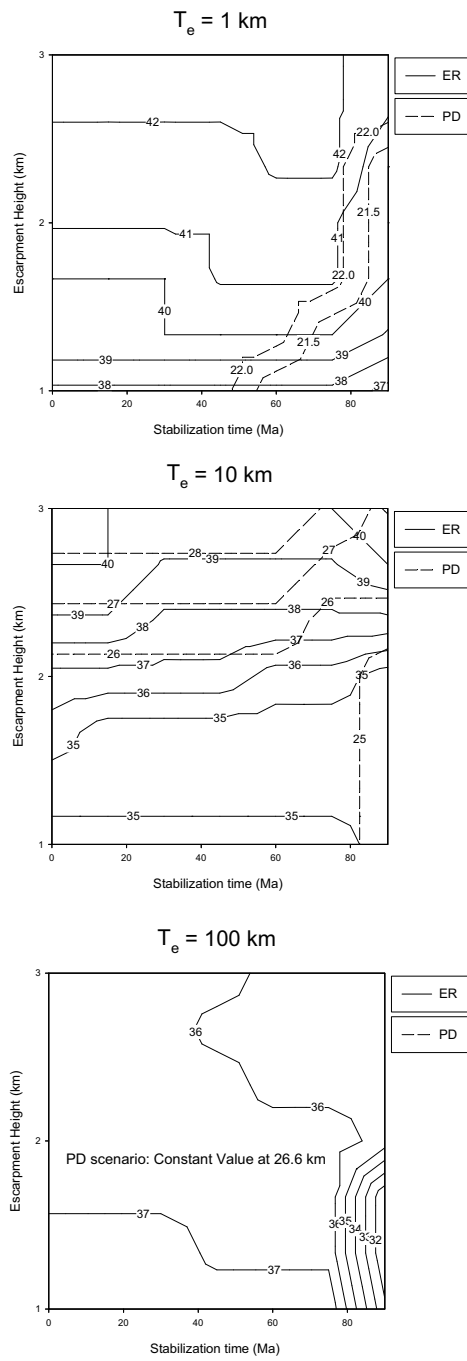
Figure 6: Distance from the coast to x_a, the location where the minimum age is predicted, as a function of escarpment height, h_0, and stabilization time, t_s, for three values of the assumed elastic plate thickness, T_e.
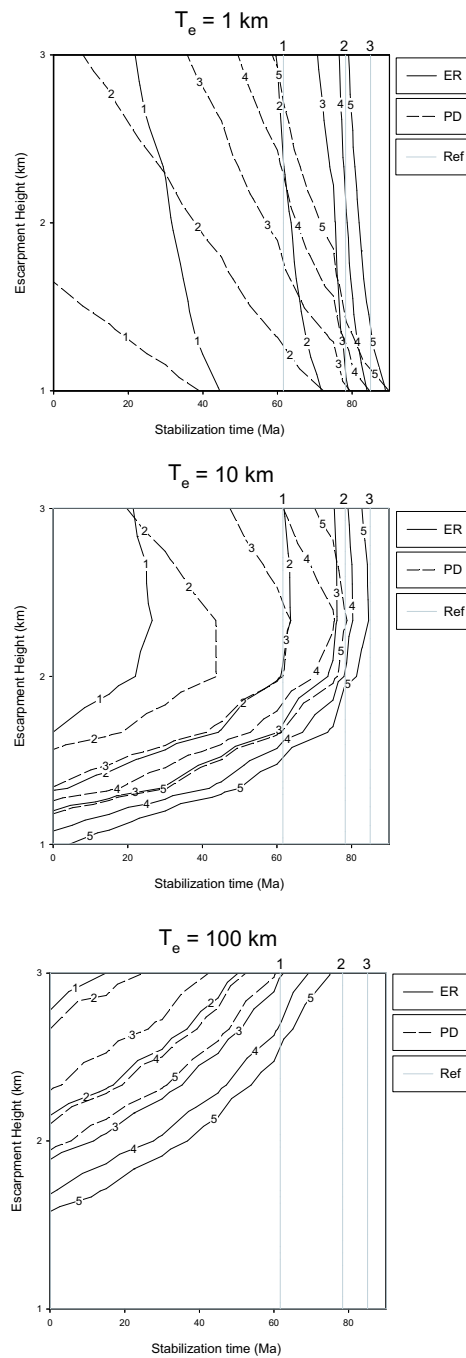
Figure 7: Slope of the distance-age relationship (in km Myr^{-1}) measured along a transect from $x = x_a$, the position of the minimum age to the coast ($x = 0$). Reference retreat rates of 1, 2 and 3 km Myr^{-1} are shown with their respective stabilization times t_s
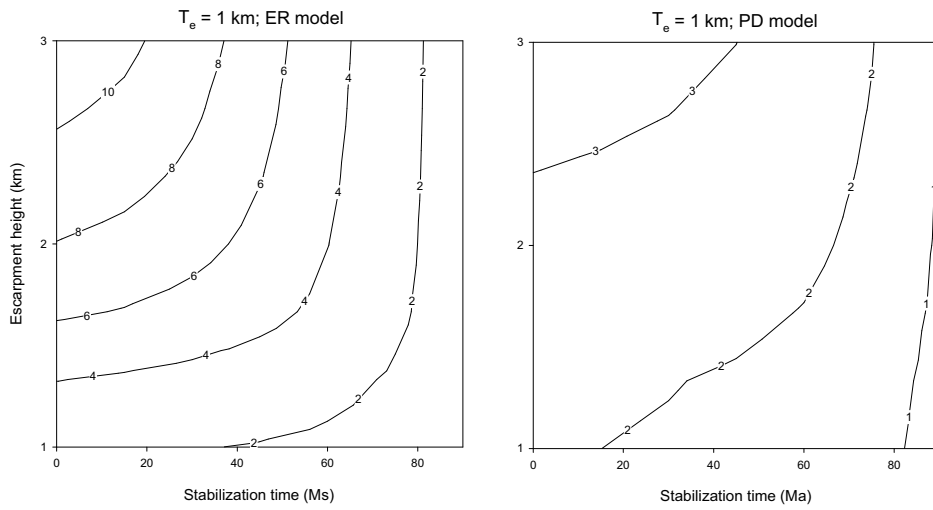
Figure 8: Ratio of local to mean exhumation rate illustrating a potential means of differentiating between the ER and PD scenarios.
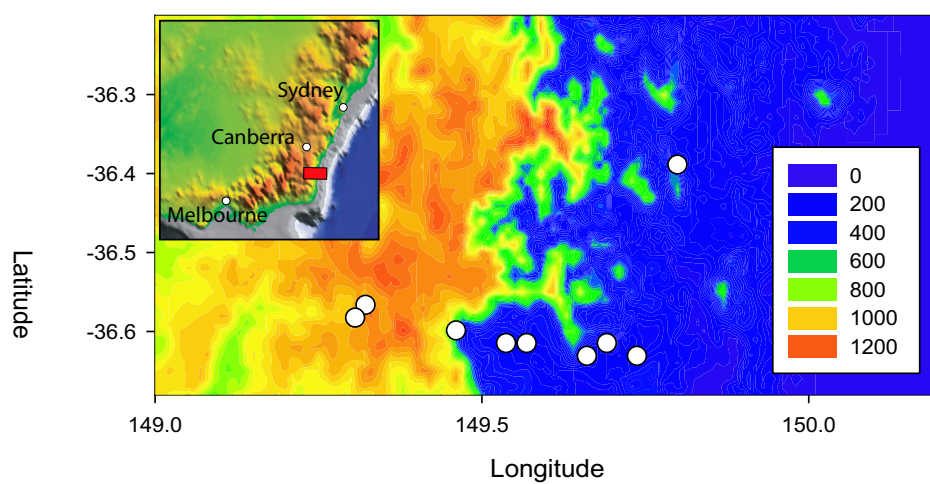
Figure 9: Topography of study area along the coast of southeastern Australia (rectangle in inset) showing the location of (U-Th)/He samples from Persano et al. (2002).
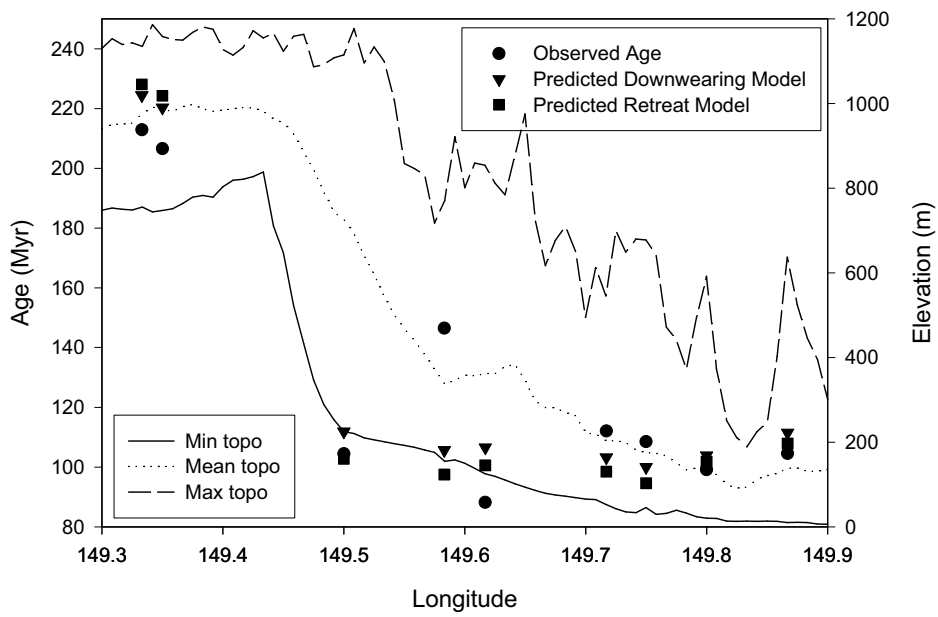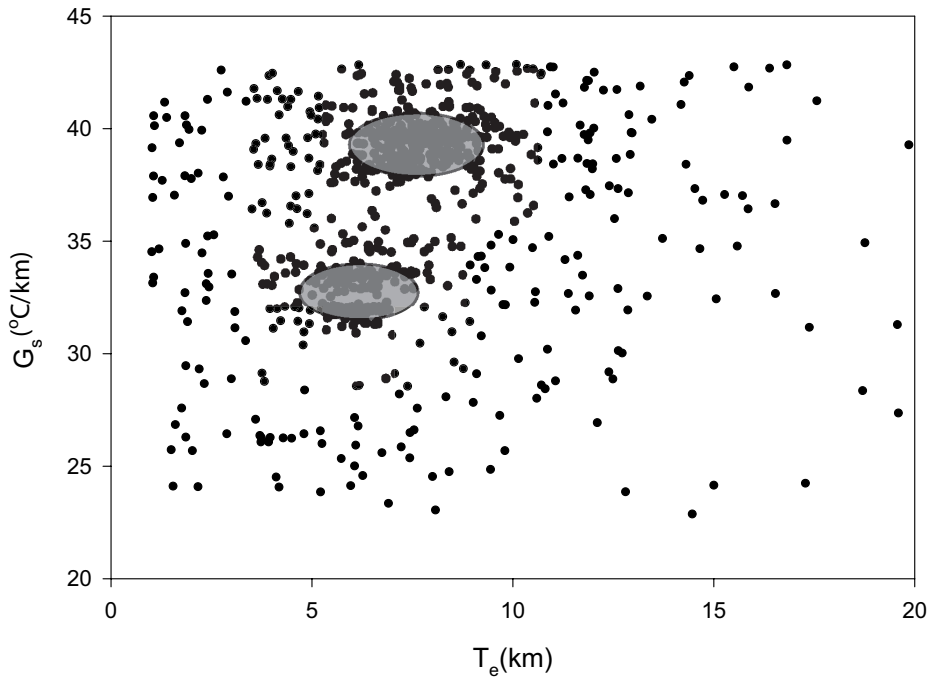
Figure 10: Observed ages across the coastal strip at the base of the southeastern Australian escarpment in southern New South Wales from Persano et al. (2002) compared to predictions of a range of models with varying scenarios and parameters.

a) Plateau Downwearing Scenario
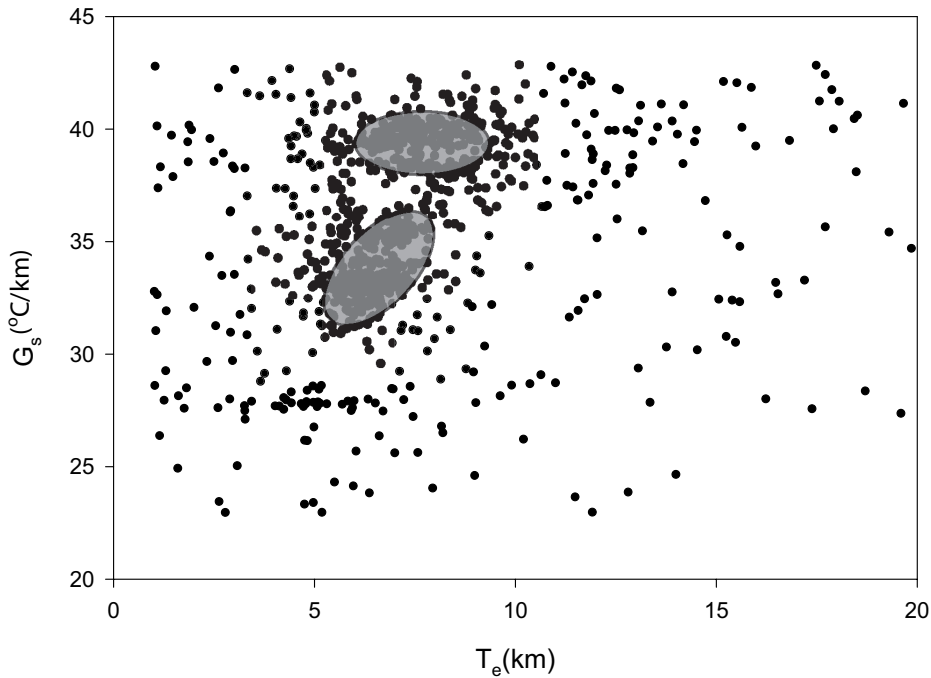

b) Escarpment Retreat Scenario

Figure 11: Location of model runs in $[T_e, T_L]$-parameter space during NA search. The grey disks correspond to the locations of local minima in misfit.
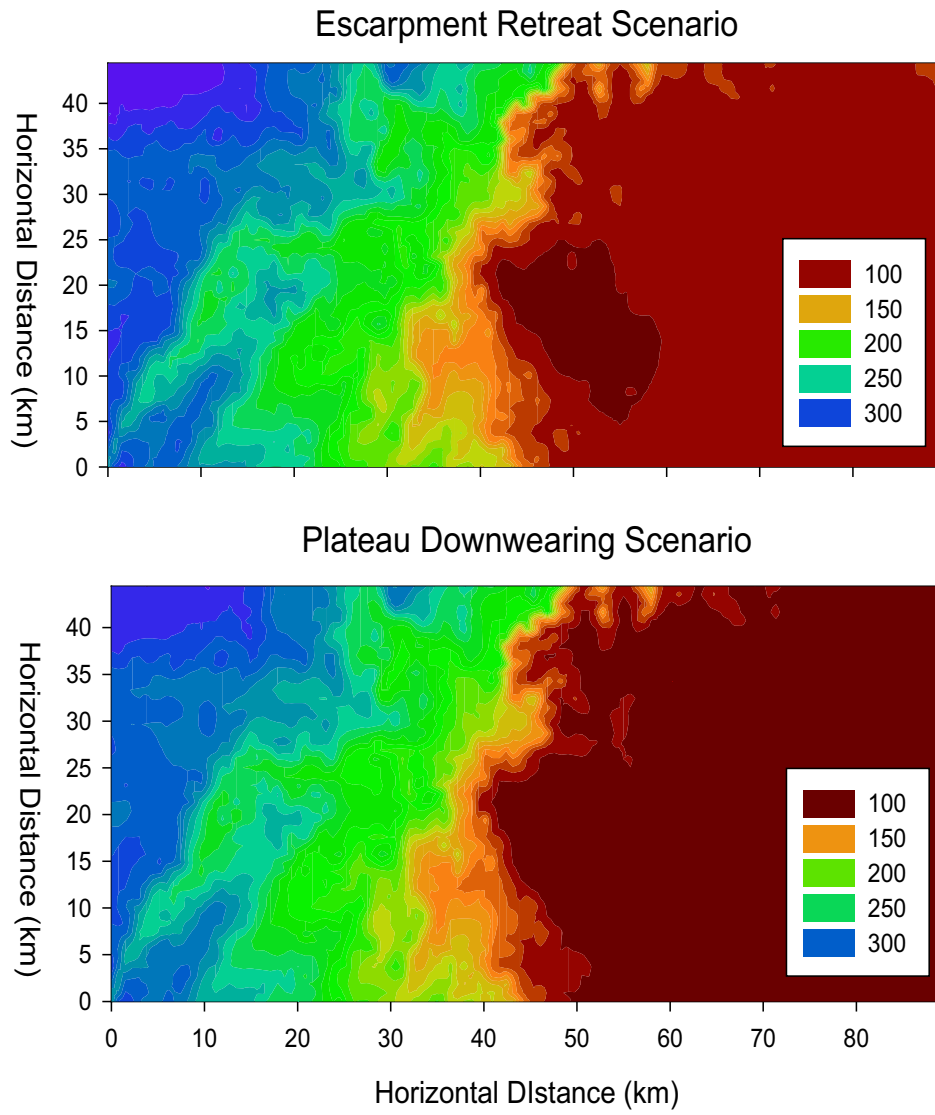
Figure 12: Predicted ages for the minimum misfit model runs assuming escarpment retreat or plateau downwearing scenario.
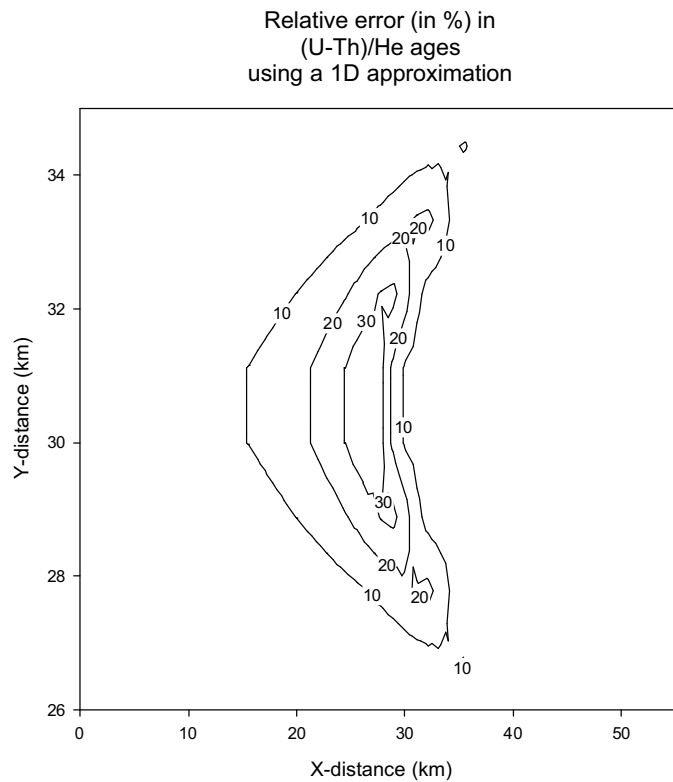
Figure 13: Relative error in predicted apatite-He ages near the base of the escarpment for a model run assuming that heat transfer is restricted to the vertical direction. Model parameters are: $h_0 = 3$ km, $w = 2$ km, $t_f = 80$ Myr, $T_e = 10$ km; model scenario is ER. These results demonstrate that ages obtained from a 1-D model of heat transfer may underestimate the true ages by as much as 40% due to the relatively large horizontal temperature gradients that exists beneath the face of an escarpment.

List of Tables

Parameter	Description	Value
$\kappa = \frac{k}{\rho c}$	Thermal diffusivity	25 km^2 Myr^{-1}
H	Heat production	0
L	Depth of base of model	35 km
W	Width of model	50 km
x_f	Final escarpment location	38 km
T_L	Temperature at base of model	885°C
T_{msl}	Temperature at mean sea level	10°C
β	Atmospheric lapse rate	0
Y	Youngs modulus	10^{11} Pa
ν	Poisson's ratio	0.25
ρ_c	Crustal density	2700 kg m^{-3}
ρ_m	Mantle (astenosphere) density	3200 kg m^{-3}

Table 1: Fixed model parameter values.